Article ID: 1003－6326(2004)03－0613－06

Mathematical modeling taking into account of intrinsic kinetic properties of cylinder-type vanadium catalyst①

CHEN Zhen-xing(陈振兴)[1], LI Hong-gui(李洪桂)[2], WANG Ling-sen(王零森)[1]
(1. State Key Laboratory of Powder Metallurgy,
Central South University, Changsha 410083, China;
2. College of Metallurgical Science and Engineering, Central South University, Changsha 410083, China)

Abstract: The method to calculate internal surface effective factor of cylinder-type vanadium catalyst Ls-9 was given. Based on hypothesis of subjunctive one dimension diffusion and combined shape adjustment factor with three-step catalytic mechanism model, the macroscopic kinetic model equation about SO_2 oxidation on Ls-9 was deduced. With fixed-bed integral reactor and under the conditions of temperature 350－410 ℃, space velocity 1 800－5 000 h^{-1}, SO_2 inlet content 7%－12%, the macroscopic kinetic data were detected. Through model parameter estimation, the macroscopic kinetic model equation was obtained.

Key words: effective factor; internal surface; model; macroscopic kinetics; catalyst
CLC number: O 643.36 **Document code:** A

1 INTRODUCTION

In the production of sulfuric acid with contact method, the effect of mass transfer on catalytic SO_2 oxidation is inevitable. Therefore, the effect of mass transfer on intrinsic kinetics needs to be investigated on the base of intrinsic kinetics. Macroscopic kinetics is very important for optimal design and optimal operation of reactor and also very important for preparation and application of vanadium catalyst, for example, selecting carrier and physical structure of diatomaceous earth, using pore maker for controlling porosity and deciding size and shape of catalyst. All of them need to know the physical process related with SO_2 oxidation. SO_2 oxidation on vanadium catalyst involves gas phase, liquid phase and solid phase. In molten salt there are many compounds combined by potassium, sodium, cesium, vanadium and sulphur, and the complex in molten salt varies with components in catalyst, temperature and reactants. Thus, it is very difficult to find out a universal mechanism model. Perhaps it is the main reason that different researchers put forward different macroscopic kinetic models[1-10].

In the previous investigations[11-14], carbonized mother liquor, ultrasonic and plasma were used to prepare catalyst Ls-9, whose activity at 410 ℃ reaches 54.7%. The alkali metals in carbonized mother liquor can reduce greatly the molten point of catalyst. Ultrasonic can modify the distribution of active components, enlarge the specific surface area and increase the concentration of crystal defect. Plasma can reduce apparently the active temperature of catalyst and shorten the active time. To lay the application foundation of Ls-9, based on analyzing the mechanism of SO_2 oxidation and considering internal diffusion, the mathematical model taking into account of intrinsic kinetic properties was deduced.

2 MATHEMATICAL MODEL OF MACROSCOPIC KINETICS

2.1 Numerical analysis of internal surface effective factor

The internal surface effective factor can be expressed with the ratio of diffusion rate of reactant on external surface to intrinsic reaction rate calculated with reactant concentration on external surface of catalyst. For column-type vanadium catalyst Ls-9(Fig. 1), the diffusion rate of O_2 on external surface is the actual reaction rate in catalyst and it can be expressed as:

$$N_{O_2,\,S} = 2\pi R_p L_p D_{eff,\,O_2}\left(\frac{\partial C_{O_2}}{\partial R}\right)_{R=R_p} + \pi R_p^2 D_{eff,\,O_2}\left(\frac{\partial C_{O_2}}{\partial L}\right)_{L=\frac{L_p}{2}} \quad (1)$$

Then, the numerical solution of internal surface effective factor can be expressed as:

$\zeta =$

① **Foundation item:** Project(20176065) supported by the National Natural Science Foundation of China
Received date: 2003－06－28; **Accepted date:** 2003－09－28
Correspondence: CHEN Zhen-xing, Professor; Tel: +86-731-8879616; E-mail: chenzx@mail.csu.edu.cn

$$\frac{2\pi R_p L_p D_{\text{eff},O_2}\left[\frac{\partial C_{O_2}}{\partial R}\right]_{R=R_p} + \pi R_p^2 D_{\text{eff},O_2}\left(\frac{\partial C_{O_2}}{\partial L}\right)_{L=\frac{L_p}{2}}}{\pi R_p^2 L_p \frac{\rho_b}{1-\varepsilon}[\hat{r}(C_{O_2})]_{R=R_p}}$$

$$= \frac{2\pi R_p L_p D_{\text{eff},O_2} \frac{1}{R_p}\frac{p}{R_g T}\left(\frac{\partial y_{O_2}}{\partial X}\right)_{X=1}}{\pi R_p^2 L_p \frac{\rho_b}{1-\varepsilon}[\hat{r}(C_{O_2})]_{X=1}} +$$

$$\frac{\pi R_p^2 D_{\text{eff},O_2} \frac{1}{R_p}\frac{p}{R_g T}\left(\frac{\partial y_{O_2}}{\partial Z}\right)_{Z=\frac{L_p}{2R_p}}}{\pi R_p^2 L_p \frac{\rho_b}{1-\varepsilon}[\hat{r}(C_{O_2})]_{X=1}}$$

$$= \frac{\left(\frac{\partial y_{O_2}}{\partial X}\right)_{X=1} + \frac{R_p}{2L_p}\left(\frac{\partial y_{O_2}}{\partial Z}\right)_{Z=\frac{L_p}{2R_p}}}{2\Phi_{O_2}^2[\hat{r}(C_{O_2})]_{X=1}} \quad (2)$$

2.2 Mathematical deduction of macroscopic kinetic equation

To obtain the numerical solution of internal surface effective factor of column-type vanadium catalyst Ls-9, Eqn. (2) needs to be simplified. For Ls-9, reaction gases diffuse along end face and sides. If catalyst is simplified as side-closed cylinder, the diffusion of reactant along sides can be neglected and only the diffusion along central axis is taken into account. For flaked differential element shown in Fig. 1, the material balance for O_2 can be carried out.

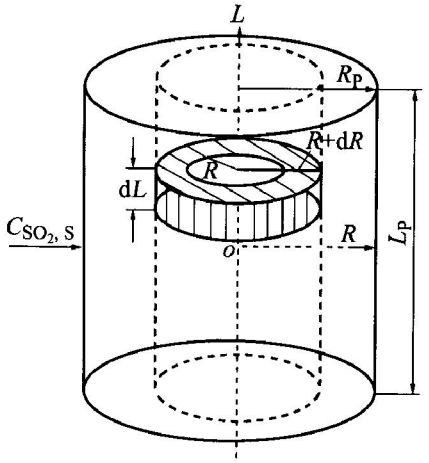

Fig. 1 Sketch of SO_2 diffusion in Ls-9

$$\frac{d^2 C_{O_2}}{dL^2} = \frac{\rho_b}{D_{\text{eff},O_2}(1-\varepsilon)}\hat{r}(C_{O_2}) \quad (3)$$

Defining $N = \frac{dC_{O_2}}{dL}$, then

$$\frac{d^2 C_{O_2}}{dL^2} = \frac{d\left[\frac{dC_{O_2}}{dL}\right]}{dL} = \frac{dC_{O_2}}{dL}\cdot\frac{d\left[\frac{dC_{O_2}}{dL}\right]}{dC_{O_2}} =$$

$$N\frac{dN}{dC_{O_2}} = \frac{\rho_b}{D_{\text{eff},O_2}(1-\varepsilon)}\hat{r}(C_{O_2})$$

$$N\,dN = \frac{\rho_b}{D_{\text{eff},O_2}(1-\varepsilon)}\hat{r}(C_{O_2})\,dC_{O_2} \quad (4)$$

Its boundary conditions are

$$L=0,\ C_{O_2}=C_{O_2,0},\ N=\left(\frac{dC_{O_2}}{dL}\right)_{L=0}=0;$$

$$L=\frac{L_p}{2},\ C_{O_2}=C_{O_2,S},\ N=\left(\frac{dC_{O_2}}{dL}\right)_{L=\frac{L_p}{2}}=N_S$$

Integrating Eqn. (4), then

$$\int_0^{N_S} N\,dN = \int_{C_{O_2,0}}^{C_{O_2,S}} \frac{\rho_b}{D_{\text{eff},O_2}(1-\varepsilon)}\hat{r}(C_{O_2})\,dC_{O_2}$$

$$\frac{1}{2}N_S^2 = \frac{\rho_b}{D_{\text{eff},O_2}(1-\varepsilon)}\left[\int_0^{C_{O_2,S}}\hat{r}(C_{O_2})\,dC_{O_2} - \int_0^{C_{O_2,0}}\hat{r}(C_{O_2})\,dC_{O_2}\right] \quad (5)$$

Because SO_2 oxidation is a rapid reaction under operation conditions and the reaction at central part of catalyst mostly reach equilibrium. Thus,

$$\int_0^{C_{O_2,0}}\hat{r}(C_{O_2})\,dC_{O_2} = 0$$

and then Eqn. (5) can be transferred into:

$$N_S = \left[\frac{dC_{O_2}}{dL}\right]_{L=\frac{L_p}{2}} = \sqrt{\frac{2\rho_b}{D_{\text{eff},O_2}(1-\varepsilon)}}\cdot \left[\int_0^{C_{O_2,S}}\hat{r}(C_{O_2})\,dC_{O_2}\right]^{1/2} \quad (6)$$

When O_2 is regarded as key component, the internal surface effective factor can be expressed as

$$\zeta = \frac{2\pi R_p L_p D_{\text{eff},O_2}\left[\frac{dC_{O_2}}{dL}\right]_{L=\frac{L_p}{2}}}{\pi R_p^2 L_p \frac{\rho_b}{1-\varepsilon}[\hat{r}(C_{O_2})]_{L=\frac{L_p}{2}}} =$$

$$\frac{2D_{\text{eff},O_2}\sqrt{\frac{2\rho_b}{D_{\text{eff},O_2}(1-\varepsilon)}}\left[\int_0^{C_{O_2,S}}\hat{r}(C_{O_2})\,dC_{O_2}\right]^{1/2}}{R_p\frac{\rho_b}{1-\varepsilon}\hat{r}(C_{O_2,S})} =$$

$$\frac{2\left(\int_0^{C_{O_2,S}}\hat{r}(C_{O_2})\,dC_{O_2}\right)^{1/2}}{R_p\sqrt{\frac{\rho_b}{2D_{\text{eff},O_2}(1-\varepsilon)}}\hat{r}(C_{O_2,S})} \quad (7)$$

Let

$$M = \frac{2}{R_p\sqrt{\frac{\rho_p}{2D_{\text{eff},O_2}(1-\varepsilon)}}}$$

then

$$\zeta = M\frac{\left(\int_0^{C_{O_2,S}}\hat{r}(C_{O_2})\,dC_{O_2}\right)^{1/2}}{\hat{r}(C_{O_2,S})}$$

$$r_{SO_2} = \zeta\cdot\hat{r}(C_{O_2,S}) = M\left(\int_0^{C_{O_2,S}}\hat{r}(C_{O_2})\,dC_{O_2}\right)^{1/2} \quad (8)$$

The oxidation of SO_2 on Ls-9 is a three-step reaction and its intrinsic mechanism model equation has been obtained in the previous research[13].

$$r_{SO_2} = \frac{K_1 p_{O_2}^{1/2}}{K_2 + K_2 p_{SO_3} + p_{SO_3}/p_{SO_2}}(1-\beta) \quad (9)$$

Because of the low pressure and high temperature in reaction system, it is suitable to assume that gases components fix with ideal gas condition equation, $p_{O_2} = C_{O_2}RT$. Then,

$$r_{SO_2} = M\left|\int_0^{C_{O_2,S}} \frac{K_1 p_{O_2}^{1/2}}{K_2 + K_3 p_{SO_3} + p_{SO_3}/p_{SO_2}} \cdot \left(1 - \frac{p_{SO_3}}{K_p p_{SO_2} p_{O_2}^{1/2}}\right) dC_{O_2}\right|^{1/2} = M\left|\int_0^{C_{O_2,S}} \frac{K_1}{K_2 + K_3 p_{SO_3} + p_{SO_3}/p_{SO_2}} \cdot \left(\sqrt{RT}\, C_{O_2}^{1/2} - \frac{p_{SO_3}}{K_p p_{SO_2}}\right) dC_{O_2}\right|^{1/2} \quad (10)$$

For SO_2 and SO_3, the inner diffusion resistance can be neglected and the concentration of SO_2 and SO_3 in tiny pores of catalyst particles approximately is equal to that of outer surface. Thus, $p_{SO_2} \approx p_{SO_2,S}$, $p_{SO_3} \approx p_{SO_3,S}$.

$$r_{SO_2} = M\left|\int_0^{C_{O_2,S}} \frac{K_1}{K_2 + K_3 p_{SO_3,S} + p_{SO_3,S}/P_{SO_2,S}} \cdot \left(\sqrt{RT}\, C_{O_2}^{1/2} - \frac{p_{SO_3,S}}{K_p p_{SO_2,S}}\right) dC_{O_2}\right|^{1/2} = \frac{2}{R_p\sqrt{\frac{\theta_b}{2D_{eff,O_2}(1-\varepsilon)}\frac{1}{RT}}} \cdot \frac{K_1 p_{O_2,S}^{3/2}}{K_2 + K_3 p_{SO_3,S} + p_{SO_3,S}/p_{SO_2,S}}\left(\frac{2}{3} - \beta\right)^{1/2} \quad (11)$$

In view of diffusion of O_2 and SO_2 along sides of cylinder-type catalyst and the ratio of side area to end face area $L_p/2R_p$, the actual reaction rate can be expressed as:

$$r_{SO_2} = \left(1 + \frac{\phi L_p}{2R_p}\right) \frac{2}{R_p\sqrt{\frac{\theta_b}{2D_{eff,O_2}(1-\varepsilon)}\frac{1}{RT}}} \cdot \frac{K_1 p_{O_2,S}^{3/2}}{K_2 + K_3 p_{SO_3,S} + p_{SO_3,S}/p_{SO_2,S}}\left(\frac{2}{3} - \beta\right)^{1/2} \quad (12)$$

where ϕ is shape adjustment factor. Actually, $\phi \approx 1$. Generally, the external diffusion resistance can be neglected and the concentration of SO_2 and SO_3 on outer surface of catalyst approximately is equal to that of gas phase bulk. Let

$$k = \left(1 + \frac{\phi L_p}{2R_p}\right) \frac{2}{R_p\sqrt{\frac{\theta_b}{2D_{eff,O_2}(1-\varepsilon)}\frac{1}{RT}}}$$

and then,

$$r_{SO_2} = k p_{O_2} \frac{K_1 p_{O_2}^{1/2}}{K_2 + K_3 p_{SO_3} + p_{SO_3}/p_{SO_2}}\left(\frac{2}{3} - \beta\right)^{1/2} \quad (13)$$

3 EXPERIMENTAL

An integral reactor was used to measure the macroscopic kinetic data. Its inner diameter is 32 mm and a thermocouple was inserted at inlet side 5 mm away from catalyst bed. In reactor, catalyst Ls-9, whose particle size is d 5 mm × 10 mm and the stacking density is 480 kg/m^3, was installed as much as 30 mL. SO_2 and air were dried with molecule sieve and active carbon respectively. After measured by rotary flowmeters, mixed and dried deeply in molecule sieve drying bottle, the mixed gas was finally fed into integral reactor. After reaction, the mixed gas was washed by concentrated sulfuric acid in gas washing bottle in order to doff SO_3 and moisture. Iodometry was used to analyze SO_2 concentration. After absorbed with NaOH solution, the remained gas was let out.

The effect of external diffusion was detected by changing space velocity. Under the same temperature and initial constitute, when the reaction rate of SO_2 varies no longer with the change of space velocity, the effect of external diffusion has been eliminated. In the experiment, the reaction rates of SO_2 at space velocities 1 800, 3 600, 5 000 and 7 000 h^{-1} were measured and the results are shown in Fig. 2. It can be concluded that under the given conditions, when the space velocity is larger than 1 800 h^{-1}, the effect of external diffusion has been eliminated.

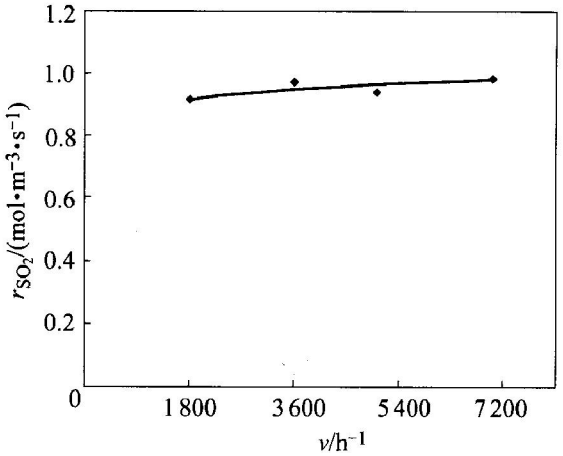

Fig. 2 Effect of space velocity on reaction rate (Innet gas SO_2 10%, reaction temperature 410 ℃)

The orthogonal design was adopted to decide the experiment conditions. For the experiment, temperature, SO_2 concentration and space velocity are the main affecting factors. Then, temperature 4 levels, 350, 370, 390 and 410 ℃, SO_2 concentration in material gas 3 levels, 7%, 9% and 11%, and space velocity 3 levels, 1 800, 3 600 and 5 000 h^{-1} were chosen. The macroscopic kinetic experimental data are shown in Table 1.

4 RESULTS AND DISCUSS

4.1 Data treatment and parameter estimation

Table 1 Macroscopic kinetic experimental data

No.	T/K	v/h^{-1}	y_{SO_2}/%	y_{O_2}/%	x/%	r_{SO_2}/(mol·m^{-3}·s^{-1})	k/(mol·m^{-3}·s^{-1}·Pa^{-1})
1	623	1800	7.03	19.5	8.07	0.145	0.215
2	623	1800	9.02	19.1	7.86	0.158	0.332
3	623	1800	11.1	18.7	5.03	0.166	0.201
4	623	3600	7.03	19.5	3.83	0.107	0.227
5	623	3600	9.02	19.1	4.18	0.122	0.107
6	623	3600	11.1	18.7	4.36	0.114	0.279
7	623	5000	7.03	19.5	2.87	0.097	0.386
8	623	5000	9.02	19.1	3.32	0.112	0.257
9	623	5000	11.1	18.7	3.18	0.099	0.413
10	643	1800	7.03	19.5	19.8	0.376	0.688
11	643	1800	9.02	19.1	20.8	0.368	0.470
12	643	1800	11.1	18.7	20.3	0.610	0.896
13	643	3600	7.03	19.5	10.5	0.176	0.537
14	643	3600	9.02	19.1	11.7	0.330	0.790
15	643	3600	11.1	18.7	10.4	0.319	0.480
16	643	5000	7.03	19.5	9.10	0.121	0.707
17	643	5000	9.02	19.1	9.35	0.314	0.552
18	643	5000	11.1	18.7	8.74	0.237	0.326
19	663	1800	7.03	19.5	52.3	0.909	0.959
20	663	1800	9.02	19.1	54.3	1.180	1.330
21	663	1800	11.1	18.7	53.8	1.450	0.729
22	663	3600	7.03	19.5	26.2	0.850	0.753
23	663	3600	9.02	19.1	27.7	0.988	0.870
24	663	3600	11.1	18.7	28.3	0.943	1.020
25	663	5000	7.03	19.5	20.5	0.568	0.957
26	663	5000	9.02	19.1	21.8	0.757	0.934
27	663	5000	11.1	18.7	23.1	0.800	0.700
28	683	1800	7.03	19.5	75.3	0.991	1.760
29	683	1800	9.02	19.1	78.3	0.827	1.950
30	683	1800	11.1	18.7	76.5	1.250	1.700
31	683	3600	7.03	19.5	48.9	0.578	2.030
32	683	3600	9.02	19.1	53.9	1.030	1.340
33	683	3600	11.1	18.7	51.6	1.070	1.710
34	683	5000	7.03	19.5	44.0	0.962	2.060
35	683	5000	9.02	19.1	46.1	1.090	2.170
36	683	5000	11.1	18.7	45.4	1.010	1.930

The reaction rate of SO_2 can be expressed as:

$$\hat{r}_{SO_2}=\frac{C_{SO_2,0}\mathrm{d}x_{SO_2}}{\mathrm{d}\left[\frac{V}{v_0}\right]}=\frac{\mathrm{d}x_{SO_2}}{\mathrm{d}\tau}C_{SO_2,0} \quad (14)$$

The actual value of reaction rate $\hat{r}_{SO_2}$ and k are shown in Table 1. Fig. 3 shows the relation of $\ln k$ with $1/T$. It is found that the tendency of $\ln k - 1/T$ is accordance with Arrhenius relation. Because R_p, L_p, ρ_b, ε and R can be regarded as constant, ϕ is in relation to radial diffusion of SO_2 and approximately equal to 1, and D_{eff,O_2} is in relation to temperature and components, k varies with the change of temperature and components and then it is probably the main reason that the relation of k and T deviates Arrhenius relation. If the change of D_{eff,O_2} with gas components is neglected, E_a and k_0 can be calculated according to Arrhenius formula: E_a= 118 176 J/mol, $k_0=3.56\times10^8$ kmol/(m^3·s·Pa). Finally, the macroscopic kinetic equation about SO_2 oxidation on Ls-9 can be obtained:

$$r_{SO_2}=3.56\times10^8 e^{-\frac{118\,176}{RT}}p_{O_2}\cdot\frac{K_1p_{O_2}^{1/2}}{K_2+K_3p_{SO_3}+p_{SO_3}/p_{SO_2}}\left(\frac{2}{3}-\beta\right)^{1/2} \quad (15)$$

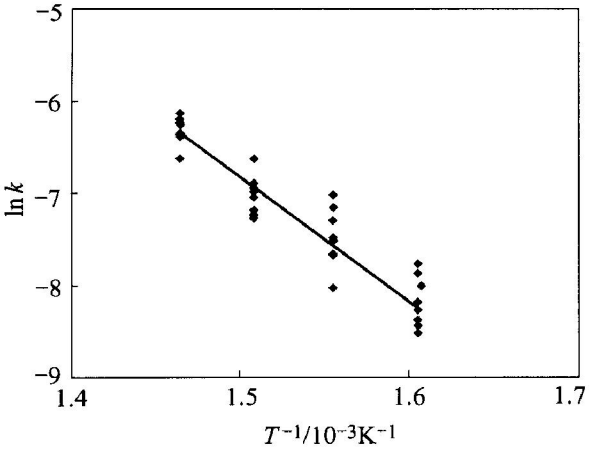

Fig. 3 Relation of $\ln k$ and $1/T$

4.2 Error analyses

According to the known characteristics of Ls-9, such as radius R_p= 25 mm, L_p= 0.01 m, $\phi\approx1$, stacking density ρ_b = 585 kg/m^3, porosity θ = 0.639, tiny pores average radius $r=4.1\times10^{-7}$ m, tortuosity δ= 4.7, bed void volume ε= 0.4, k_C can be calculated according to Eqn. (13). Then the reaction rate r_{CO_2} can be calculated according to Eqn. (15). Fig. 4 shows the relative error S_i between the actual reaction rate $\hat{r}_{SO_2}$ and the calculated reaction rate r_{SO_2}. The relative errors distribute uniformly in the vicinity of S_i= 0 and it show that the macroscopic kinetic model equation fits in with experimental results well.

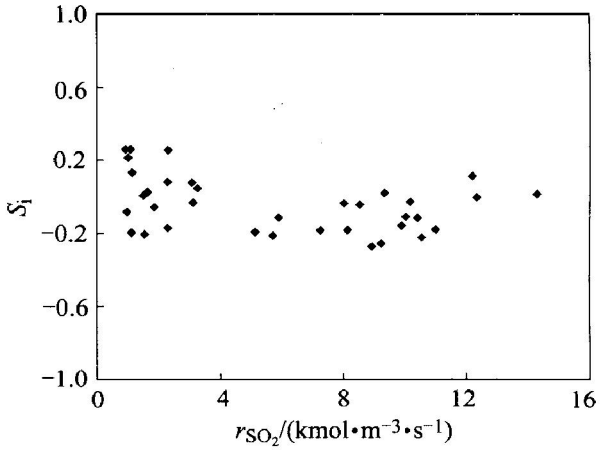

Fig. 4 Error distribution

5 CONCLUSIONS

1) The numerical solution of internal surface effective factor for cylinder-type catalyst Ls-9 was given:

$$\zeta=\frac{\left(\frac{\partial y_{O_2}}{\partial X}\right)_{x=1}+\frac{R_p}{2L_p}\left(\frac{\partial y_{O_2}}{\partial Z}\right)_{Z=\frac{L_p}{2R_p}}}{2\phi_{O_2}^2[\hat{r}(C_{O_2})]_{x=1}}$$

2) Based on the hypothesis of subjunctive one dimension diffusion of reactant in cylinder-type catalyst and combined shape adjustment factor with three-step catalytic mechanism model, the macroscopic kinetic model equation about SO_2 oxidation on Ls-9 was obtained as:

$$r_{SO_2}=\left(1+\frac{\phi L_p}{2R_p}\right)\frac{2}{R_p\sqrt{\frac{\rho_b}{2D_{eff,O_2}(1-\varepsilon)}\frac{1}{RT}}}\cdot\frac{K_1p_{O_2,S}^{3/2}}{K_2+K_3p_{SO_3,S}+p_{SO_3,S}/p_{SO_2,S}}\left(\frac{2}{3}-\beta\right)^{1/2}$$

3) The macroscopic kinetic data about SO_2 oxidation on Ls-9 were detected with fixed bed integral reactor under the condition of 350 - 410 ℃, space velocity 1 800 - 5 000 h^{-1} and inlet concentration of SO_2 7% - 12%. Model parameters were estimated and then simple formula of macroscopic kinetic equation was obtained:

$$r_{SO_2}=3.56\times10^8 e^{-\frac{118\,176}{RT}}p_{O_2}\cdot\frac{K_1p_{O_2}^{1/2}}{K_2+K_3p_{SO_3}+p_{SO_3}/p_{SO_2}}\left(\frac{2}{3}-\beta\right)^{1/2}$$

4) The macroscopic kinetic model equation fits the experiment data well.

Nomenclature

C_{O_2} —O_2 concentration, kmol·m^{-3};

$C_{O_2,0}$ —O_2 concentration in the center of cata-

lyst, kmol·m^{-3};

$C_{O_2,S}$ —O_2 concentration on the surface of catalyst, kmol·m^{-3};

$C_{SO_2,S}$ —SO_2 concentration on the surface of catalyst, kmol·m^{-3};

D_{eff,O_2} —effective diffusion coefficient of O_2, m^2·s^{-1};

K_1, K_2, K_3 —reaction rate constants;

K_p —chemical equilibrium constant of reaction $SO_2+\frac{1}{2}O_2 \rightleftharpoons SO_3$, Pa$^{-1/2}$;

L_p —length of catalyst, m;

$N_{O_2,S}$ —diffusion rate of O_2 on the surface of catalyst, kmol·s^{-1};

p —total pressure of gas, Pa;

p_{O_2}, p_{SO_2}, p_{SO_3} —fractional pressure of O_2, SO_2 and SO_3 respectively, Pa;

R_g —general gas constant, J·kmol^{-1}·K^{-1};

R_p —radius of catalyst, m;

$\hat{r}(C_{O_2})$ —calculated reaction rate of O_2, kmol·kg^{-1}·s^{-1};

r_{SO_2} —calculated reaction rate of SO_2, kmol·m^{-3}·s^{-1};

$\hat{r}_{SO_2}$ —actual reaction rate of SO_2, kmol·m^{-3}·s^{-1};

T —reaction temperature, K;

V —volume of reactor, m^3;

v_0 —SO_2 flux at the inlet of reactor, m^3·s^{-1};

x —conversion of SO_2, %;

X —dimensionless radius of catalyst, $X=R/R_p$;

y_{O_2}, y_{SO_2}, y_{SO_3} —mole fraction of O_2, $SO_2$and SO_3 respectively, %;

Z —dimensionless length of catalyst, $Z=L/R_p$;

ζ —internal surface effective factor;

ρ_b —bulk density of catalyst, m^3·kg^{-1};

ε —void volume, %;

ϕ_{O_2} —thiele module,

$$\phi_{O_2}=\frac{V_P}{S_P}\sqrt{\frac{R_gT}{P}\frac{\rho_b}{D_{eff,O_2}(1-\varepsilon)}}=\frac{R_p}{2}\sqrt{\frac{R_gT}{P}\frac{\rho_b}{D_{eff,O_2}(1-\varepsilon)}},\ \text{dimensionless;}$$

β —dimensionless, $\beta=\frac{p_{SO_3}}{K_P p_{SO_2} p_{O_2}^{1/2}}$;

ψ —shape adjustment factor, dimensionless;

v —space velocity, h^{-1};

τ —space time, h.

REFERENCES

[1] Dunn J P, Koppula P R, Stenger H G, et al. Oxidation of sulfur dioxide to sulfur trioxide over supported vanadia catalysts[J]. Applied Catalysis B: Environmental, 1998, 19(2): 103-117.

[2] Eriksen K M, Karydis K A, Boghosian S, et al. Deactivation and compound formation in sulfuric acid catalysts and model systems[J]. Journal of Catalysis, 1995, 155(1): 32-42.

[3] Masters S G, Chrissanthopoulos A, Eriksen K M, et al. Catalytic activity and deactivation of SO_2 oxidation catalysts in simulated power plant flue gases[J]. Journal of Catalysis, 1997, 166(1): 16-24.

[4] Adlkofer J, Dieckmann E, Winkler E. Catalysts for high-concentration SO_2 gases[J]. Sulphur, 1993, 229: 50-52.

[5] Ruoyu H, Xin L, Hongzhong L, et al. Modeling and simulation of SO_2 oxidation in a fixed-bed reactor with periodic flow reversal[J]. Catalysis Today, 1997, 38(1): 47-58.

[6] Silveston P L, Hudgins R R, Bogdashev S, et al. Modelling of a periodically operating packed-bed SO_2 oxidation reactor at high conversion[J]. Chemical Engineering Science, 1994, 49(3): 335-339.

[7] Vernikovskaya N V, Zagoruiko A N, Noskov A S. SO_2 oxidation method. Mathematical modeling taking into account dynamic properties of the catalyst[J]. Chemical Engineering Science, 1998, 54(20): 2089-2094.

[8] Alvarez E, Blanco J, Knapp C. Pilot plant performance of a SO_2 to SO_3 oxidation catalyst for flue-gas conditioning [J]. Catalysis Today, 2000, 59(3): 417.

[9] Rosendall B, Finlayson B A. Transport effects in packed-bed oxidation reactors[J]. Computers & Chemical Engineering, 1995, 19(11): 1207-1212.

[10] Dunn J P, Stenger H G, Wachs I E. Oxidation of sulfur dioxide over supported vanadium catalysts: molecular structure-reactivity relationships and reaction kinetics [J]. Catalysis Today, 1999, 51(2): 301-309.

[11] CHEN Zhen-xing, HUANG Qiao-ping. Effect of alkaline metals on low temperature activity of vanadium catalyst[J]. Chemical Journal on Internet, 2002, 4(9): 42-47.

[12] CHEN Zhen-xing, YANG Gang, YE Hua. Preparation of Cs-Rb-V series sulphuric acid catalyst[J]. Trans Nonferrous Met Soc China, 2001, 11(4): 595-598.

[13] CHEN Zhen-xing, YE Hua, LIU Jin, et al. Mechanism explanation for SO_2 oxidation rate of Cs-Rb-V sulfuric acid catalyst at low temperature[J]. Trans Nonferrous Met Soc China, 2001, 11(3): 462-465.

[14] CHEN Zhen-xing, LI Hong-gui, WANG Ling-sen. Activity enhancement of vanadium catalyst with ultrasonic preparation process for the oxidation of sulfur dioxide [J]. Journal of Natural Gas Chemistry, 2003, 12(2): 139-144.

(Edited by YUAN Sai-qian)